Screening of sphingolipid metabolism-related genes associated with immune cells in myocardial infarction: a bioinformatics analysis

Jijuan Wang[1#], Ping Wang[2#], Weihua Wang[3], Huiling Jin[4]

[1]Department of Cardiovascular Medicine, The Second Affiliated Hospital of Guangzhou University of Traditional Chinese Medicine, Guangzhou, China; [2]Department of critical medicine, Shenzhen Hospital of Beijing University of traditional Chinese medicine (Longgang), Shenzhen, China; [3]Guangzhou Xidai Hemodialysis Center Co., Ltd., Guangzhou, China; [4]Department of Cardiovascular Diseases, Affiliated Hospital of Shanxi University of Chinese Medicine, Taiyuan, China

Contributions: (I) Conception and design: W Wang; (II) Administrative support: W Wang, H Jin; (III) Provision of study materials or patients: J Wang; (IV) Collection and assembly of data: P Wang, H Jin; (V) Data analysis and interpretation: All authors; (VI) Manuscript writing: All authors; (VII) Final approval of manuscript: All authors.

[#]These authors contributed equally to this work.

Correspondence to: Huiling Jin, MD. Department of Cardiovascular Diseases, Affiliated Hospital of Shanxi University of Chinese Medicine, Taiyuan, China. Email: 304856538@qq.com.

Background: Inflammation and immune cell infiltration in infarcted myocardial tissue are critical to myocardial infarction (MI) prognosis, and alterations in sphingolipid metabolism (SM) have been shown to potentially influence the inflammatory response and induce cardioprotection, but the underlying mechanisms are unclear. We therefore performed bioinformatics analysis to screen for key genes of SM in MI immune cells.

Methods: Three matrix files including GSE61145, GSE23294, and GSE71906 were downloaded from the Gene Expression Omnibus (GEO) database. GSE61145 was a human peripheral blood database, and GSE23294 and GSE71906 were 2 mouse myocardial tissue databases. R and annotation packages were used to screen for differentially-expressed genes (DEGs). Datasets of human and mouse cardiac tissues were downloaded from the GEO database for subsequent validation. The downloaded platform and matrix files were processed using R language and annotation packages. Key targets and enrichment pathways were identified using Gene Ontology (GO) term enrichment and Kyoto Encyclopedia of Genes and Genomes (KEGG) pathway analysis. The Wilcoxon test was performed on the genes involved in SM pathways in neutrophils.

Results: A total of 261 DEGs were obtained from human peripheral blood datasets, among which 101 were immune-related. GO analysis revealed that neutrophil activation, T cell activation, and T cell differentiation were significantly enriched in the immune-related DEGs. Three types of immune cells were identified in infarcted myocardial tissues. In addition, 194 DEGs were obtained from mouse myocardial tissue data, among which 6 SM-related genes (*Asah1*, *Degs1*, *Neu1*, *Sptlc2*, *Sphk1*, and *Gba2*) were significantly associated with MI. Evaluation of the relationships between these DEGs and neutrophils showed that the expression of the *Sptlc2* gene was significantly upregulated in neutrophils of the MI group, while the expression levels of the *Asah1* and *Degs1* genes were downregulated.

Conclusions: We identified 3 SM-related genes that were highly associated with neutrophils in MI, which may advance our understanding of SM in immune cells after MI.

Keywords: Immune system; neutrophils; sphingolipid metabolism; myocardial infarction (MI)

Introduction

Myocardial infarction (MI) is a cardiovascular event caused by prolonged severe myocardial ischemia and ischemic necrosis due to a sharp reduction or interruption of coronary blood supply (1). The main clinical presentation of MI is typical ischemic chest discomfort, which can be accompanied by nausea, vomiting, sweating, dyspnea, and/or syncope (2). In the United States, the overall prevalence of MI among adults over the age of 20 is 3%. Every 40 s about 1 American develops MI. MI is also one of the leading causes of mortality worldwide. With a 5-year survival rate of approximately 30%, MI has a tremendous impact on health and the global economy (3). The degree of MI is positively associated with the risk of developing heart failure after infarction, during which ventricular remodeling is a prominent pathophysiological process (4). The immune system is particularly important after MI (5). The pro-inflammatory response triggered by MI can clear necrotic cells and debris; if over-activated, however, it causes severe damage to the extracellular matrix (6). Therefore, the inflammatory response plays a dual role in MI prognosis. Maintaining the balance of the inflammatory response is crucial for improving cardiac prognosis and protecting ventricular function. Activation of various immune cells (e.g., neutrophils, lymphocytes, monocytes, and macrophages) and their infiltration into tissues after MI have been demonstrated (7), but are still under investigation. Therefore, targeting the immune system and resolving inflammation may be a therapeutic option for cardioprotection after MI.

The immune system is involved in complex physiological processes. Serving as a keeper of dynamic balance (8,9), it senses and integrates environmental signals by recruiting various immune cells and responds to different pathological circumstances, thus ensuring cell viability and long-term survival. The immune response to various challenges results in dramatic changes involving numerous signaling molecules and intricate cell-to-cell interactions (10). Sphingolipid metabolites (SMs), in particular ceramide (N-acyl-sphingosine), ceramide-1-phosphate (C1P), and sphingosine-1-phosphate (S1P), are bioactive lipid molecules that have been shown to regulate a wide variety of cellular processes and play key roles in immunity, inflammation, and inflammatory diseases (11). Composed of ceramides and various types of glycolipids, SMs are ubiquitous components in eukaryotic membranes. They serve as an important second messenger in immune cells and play key roles in cellular signal transduction. S1P, a key mediator of SM, is involved in regulating cell proliferation, differentiation, and survival. Ceramide is a key precursor to bioactive SMs and transmits intracellular signals during cell cycle arrest, apoptosis, autophagy, and death (12). While some targets of sphingolipid signaling have been identified, how it modulates immune responses remains unknown. A large body of evidence suggests that SM plays an important regulatory role in MI. Blood ceramide level can be marked as a predictor of the severity of cardiovascular complications and mortality (13). It was found that the S1P/ceramide ratio in the non-infarcted area of the left ventricle of MI rats was significantly decreased, suggesting that the early activation of apoptosis in the non-infarcted area of the left ventricle after MI may be related to a decreased ratio (14). Pharmacological elevation of bioactive lipids after acute MI leads to improvements in cardiac structure and function (15). Hadas *et al.* (16) suggested that acid ceramidase attenuated detrimental neutrophil levels and cell death in the left ventricle after MI by altering SM, and inhibition of ceramide *de novo* synthesis could reduce myocardial reperfusion injury and inflammation (17). In a lipidomic study, the expression of ceramide kinase, which phosphorylates ceramide to produce C1P, was found to be consistently upregulated in myocardial tissue after MI (18).

In our current study, we utilized bioinformatics technology to investigate MI-related genes and immune mechanisms, provided further insights into the roles of SMs in the immune system and their interactions, and attempted to explain the possible roles of SM-related genes in disease progression after MI. We present the following article in accordance with the STREGA reporting checklist (available at https://jtd.amegroups.com/article/view/10.21037/jtd-22-1041/rc).

Methods

Identification of differentially-expressed genes (DEGs) in the Gene Expression Omnibus (GEO) dataset

GSE61145 is a human peripheral blood dataset and GSE23294 and GSE71906 are 2 mouse myocardial tissue datasets. All datasets were selected from the GEO database. GSE61145 includes 7 normal myocardial tissues and 17 MI specimens, whereas GSE23294 and GSE71906 contain 10 normal myocardial tissues and 10 MI specimens. We

downloaded the platform and matrix files and processed them using the R package and annotation packages. The probe names were converted to the international standard names (gene symbols) for the genes. MI and normal samples from 3 microarray datasets were screened using BioConductor (http://www.bioconductor.org/), setting the |fold change (FC)| as ≥0.75 and the adjusted P value cutoff as <0.05 for the screening of DEGs. The 3 DEG datasets were integrated by batch normalization in R. We obtained upregulated and downregulated genes in these 3 profiles for subsequent analyses. The study was conducted in accordance with the Declaration of Helsinki (as revised in 2013).

Gene Ontology (GO) and Kyoto Encyclopedia of Genes and Genomes (KEGG) enrichment analyses

To gain a deeper understanding of the selected DEGs and key modules, the Database for Annotation, Visualization, and Integrated Discovery (DAVID) (19) was used for the GO and KEGG enrichment analyses (20), during which a pathway database containing information on how molecules or genes are networked was applied, with the adjusted P value cutoff being <0.05. Immune network pathways were identified using the Cytoscape plugin ClueGO.

Assessment of immune cell infiltration

The gene expression levels in the integrated dataset were normalized using a format acceptable to "Cell type Identification By Estimating Relative Subsets Of RNA Transcripts (CIBERSORT)" and then the data were uploaded to the CIBERSORT web portal (http://cibersort.stanford.edu/), which quantifies cell composition from bulk gene expression profiles (GEPs) (21). The types of infiltrating immune cells were predicted using the CIBERSORT algorithm (P value <0.05). To analyze the significant differences in immune cell expression levels among different cell types,

Verification of SM-related gene expression in neutrophils in the single-cell sequencing database GSE130699

The MI mouse single-cardiomyocyte RNA sequencing dataset (GSE130699) was downloaded from the GEO database. A total of 2 normal and 2 MI samples were included. MI was induced in neonatal mice on the 1st or

8th day after birth by permanent ligation of the anterior descending coronary artery, and myocardial tissue was collected on the 1st and 3rd days after the operation. The surgery was regarded as successful after TTC staining confirmed the death of myocardial cells. After annotation, the cell types were identified in the normal group and the modeling group.

Statistical analysis

Data were analyzed using SPSS 22.0 software. The differences in SM-related gene expression levels in neutrophils were compared using the Wilcoxon rank sum test. $P<0.05$ was considered to represent statistical significance.

Results

Identification of 101 immune-related DEGs

To gain a comprehensive understanding of MI genomic expression profiles, the MI expression profile dataset (GSE61145) was normalized, and a total of 181 upregulated and 80 downregulated genes were screened (Table S1). *Figure 1A* is the volcano plot of DEGs in this dataset, in which 101 immune-related DEGs were identified. Immune genes were significantly enriched in biological processes including neutrophil migration, T cell activation, and T cell differentiation (*Figure 1B*). After screening by CIBERSORT, 7 normal peripheral blood samples and 17 MI peripheral blood samples were obtained. Three types of immune cells were identified, namely neutrophils, resting memory CD4+ T cells, and γδ T cells (*Figure 1C*).

GO functional and KEGG pathway enrichment analysis of 185 upregulated genes and 9 downregulated genes

To gain insight into MI genomic expression profiles, 2 additional mouse MI expression profile datasets (GSE23294 and GSE71906) were normalized, and a total of 185 upregulated and 9 downregulated genes were screened (Table S2). *Figure 2A* is a volcano plot for these 2 datasets. In addition, a heatmap was used to plot the top 15 upregulated and downregulated genes, as shown in *Figure 2B*. These genes included *Sprr1a*, *Adamts4*, *Fstl3*, *Hmox1*, *Cdr2*, *Empl*, *Anxa2*, *Ctgf*, *Col4a1*, *Tpm4*, *Timp1*, *Uck2*, *Rcan1*, *Tubb6*, and *Actn1*.
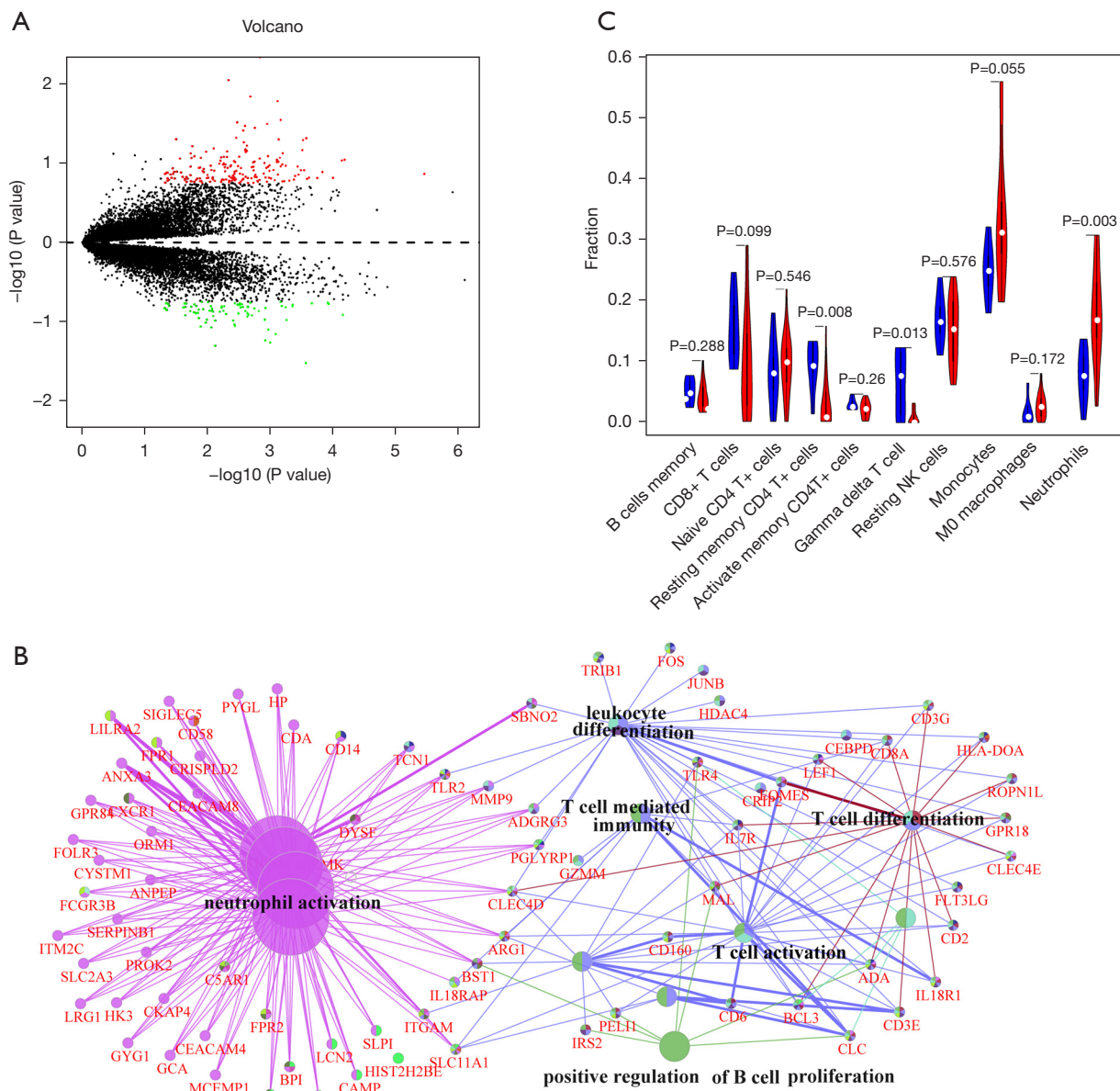
2990

Wang et al. Sphingolipid metabolism in immune cells

Figure 1 DEGs in MI. (A) Volcano plot of DEGs (black dots represent all DEGs, red dots represent upregulated DEGs and green dots represent downregulated DEGs). (B) GO analysis of immune-related cells and infiltrating immune cells in 101 MI patients. (C) Violin plot of the proportions of 10 immune cells in MI and normal tissue (blue represents normal tissue and red represents inflamed tissue). DEGs, differentially-expressed genes; GO, Gene Ontology; MI, myocardial infarction.

To further understand these 2 mouse DEGs datasets, we performed GO functional and KEGG pathway enrichment analyses for DEGs using the DAVID database. Different genes were particularly abundant in biological processes including response to stress, response to external stimulus, inflammatory response, extracellular space, extracellular region part, cell migration, defense response, extracellular region, wound healing, and response to wounding (*Figure 2C*). Pathways involving different genes are shown in *Figure 2D*, including the cell cycle, IL-17 signaling pathway, amoebiasis, ECM-receptor interaction, cytokine-cytokine receptor interaction, Salmonella infection, phagosome, legionellosis, chemokine signaling pathway, and osteoclast differentiation.
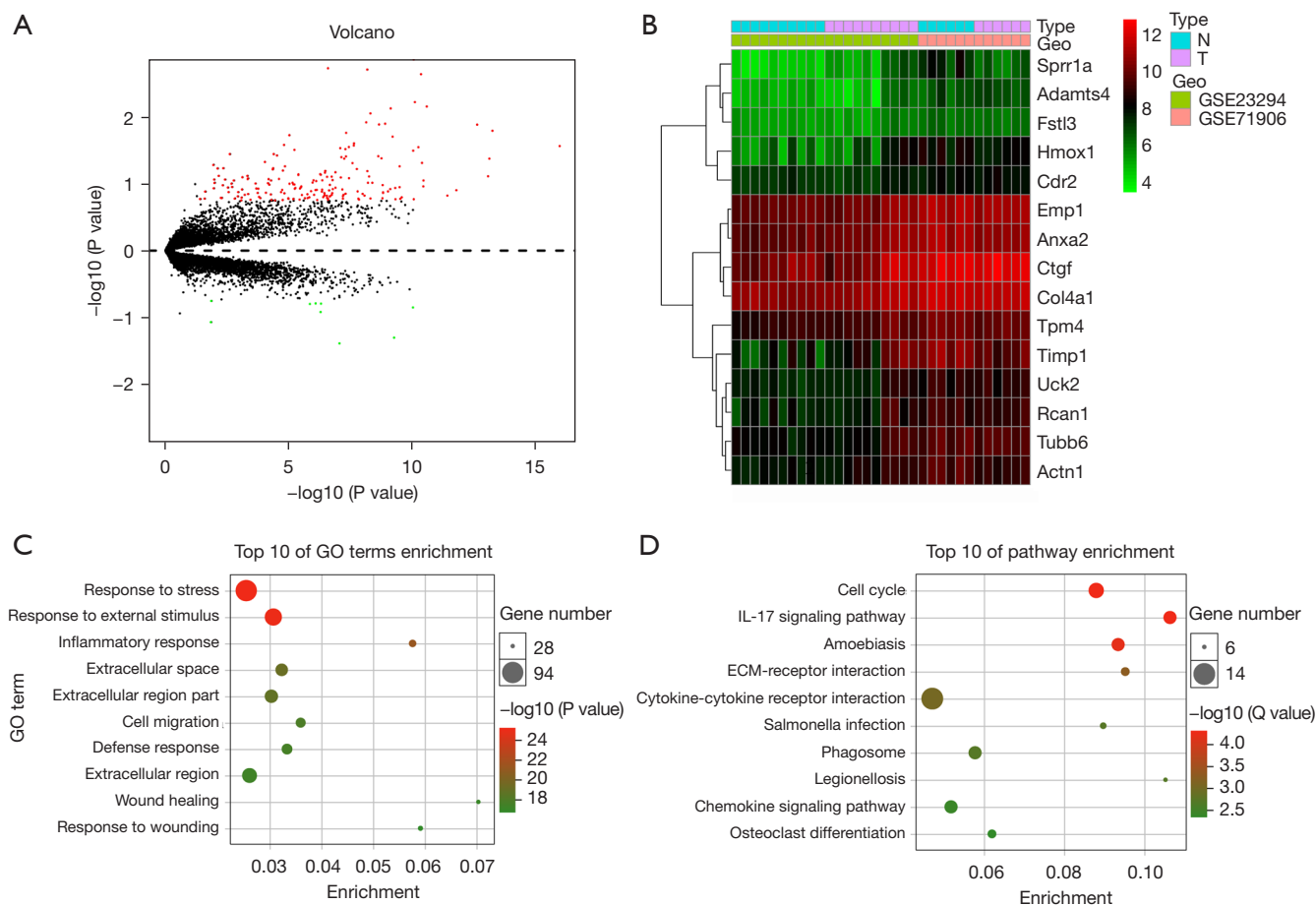
Figure 2 The top 10 biological processes and enriched biological pathways of DEGs in MI. (A) Volcano plot of DEGs (black dots represent all DEGs, red dots represent upregulated DEGs and green dots represent downregulated DEGs); (B) top 15 upregulated and downregulated genes (red represents upregulated DEGs and green represents downregulated DEGs); (C) top 10 enriched GO terms; (D) top 10 enriched pathways. The ordinate is the top 10 significantly enriched GO terms and KEGG pathways, and the abscissa is the enrichment factor. The size of the bubble represents the number of DEGs in the functional area. GO, Gene Ontology; ECM, extracellular matrix; DEGs, differentially-expressed genes; MI, myocardial infarction; KEGG, Kyoto Encyclopedia of Genes and Genomes.

Expression of SM-related genes in myocardial tissues

We analyzed the differences in SM-related genes obtained from GSE23294 and GSE71906 in myocardial tissues of MI mice. Among them, the expression levels of *Asah1*, *Degs1*, *Neu1*, *Sptlc2*, and *Sphk1* were significantly upregulated, and the expression level of *Gba2* was downregulated (*Figure 3*).

Differential expression of SM-related genes in neutrophils

Identification of DEGs from expression profiles by microarrays (GSE611145, GSE23294, and GSE71906) reflects the average differential expression of genes in multiple cells, whereas single-cell sequencing can reflect the genomic and transcriptomic statuses of individual cells. Furthermore, we analyzed the differential expression of SM-related genes screened in myocardial tissue obtained from GSE130699. After annotation, 12 distinct cell populations were identified from the single-cell sequencing data (*Figure 4*). A total of 3,896 neutrophils were recorded. The normal group included 657 neutrophils and the MI group included 3239 neutrophils. The expression levels of *Asah1*, *Degs1*, and *Sptlc2* were significantly different in neutrophils (*Figure 5*). Notably, the expression of *Sptlc2* was significantly upregulated in neutrophils of the MI group, while the expression levels of *Asah1* and *Degs1* were downregulated.
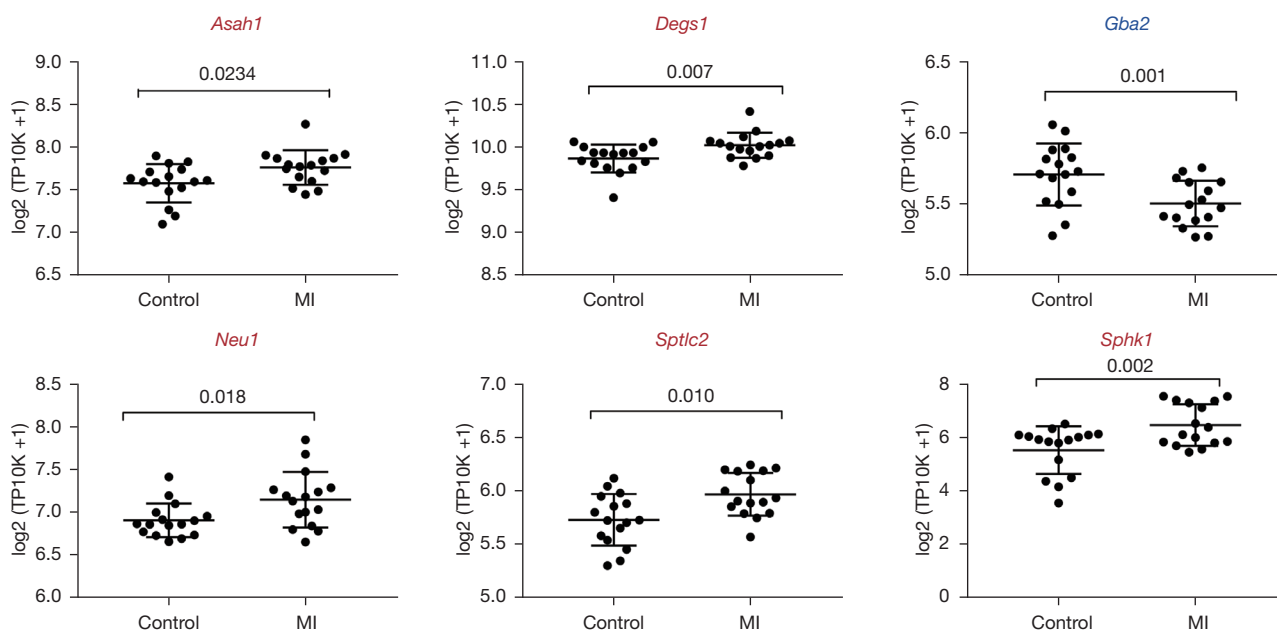
2992

Wang et al. Sphingolipid metabolism in immune cells

Figure 3 Different expression levels of screened SM-related genes in MI mice and healthy controls. Red represents upregulated genes and blue represents downregulated genes. SM, sphingolipid metabolism; MI, myocardial infarction.
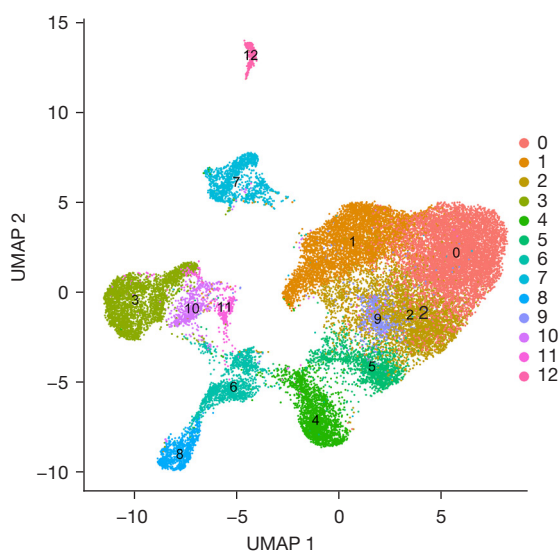

Figure 4 Different cell populations from GSE130699. After genetic marking, UMAP clustering was used to cluster cells into different datasets. UMAP, uniform manifold approximation and projection.

Discussion

A variety of immune cells, inflammatory cytokines, enzymes, lipid mediators, and cellular molecules participate in the occurrence and development of MI via complex mechanisms. Our data showed that some genes were significantly enriched in immune regulation. Subsequent analyses also revealed that neutrophils and T cells are involved in MI. Among immune cells, neutrophils, which are a type of polymorphonuclear leukocyte, are considered as a major player in the innate immune system and are also the first leukocytes recruited to the sites of acute inflammation for clearing infection (22,23). In another study, however, neutrophils played further roles in chronic inflammatory conditions and in adaptive immune responses (24). A study in SM has shown that both ceramides and S1P are involved in the regulation of neutrophil recruitment, phagocytosis, and migration (25). As pro-apoptotic metabolites, they also mediate neutrophil apoptosis through caspase activation (26). T cells are another type of immune cell. As the main trigger of many types of inflammation, they consist of multiple subpopulations that play different roles at different life stages and have the potential to recognize antigens, maintain immune memory, and develop self-tolerance (27). A study has found that acid sphingomyelinase-dependent ceramide signaling plays a key role in mediating the activation, proliferation, and response of CD4+ T cells (28). Furthermore, a study has shown that targeting macrophages can prevent left ventricular
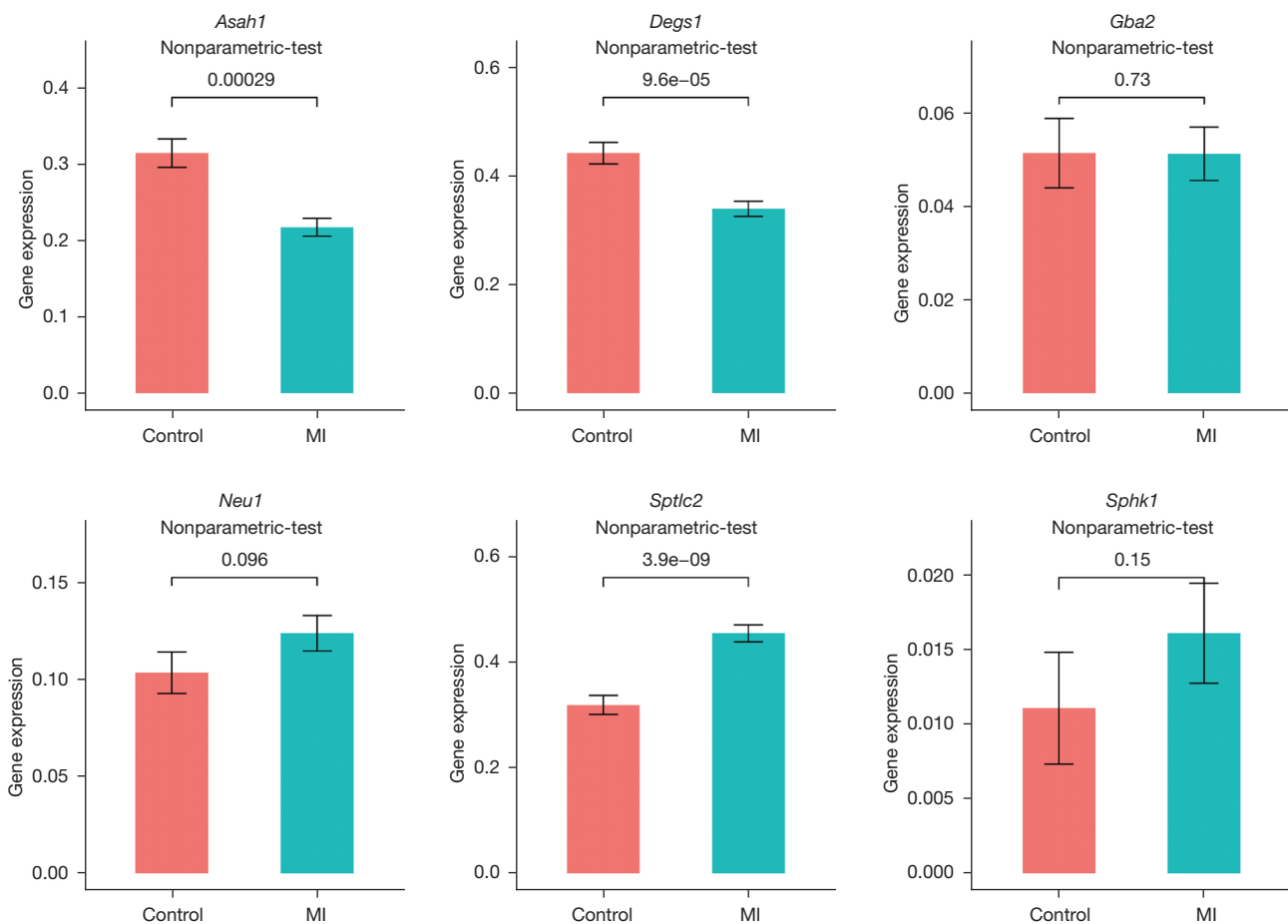
Figure 5 Screening for the differential expression of SM-related genes in neutrophils. DEGs were compared between the normal and MI groups in the single-cell dataset GSE130699. SM, sphingolipid metabolism; DEGs, differentially-expressed genes; MI, myocardial infarction.

remodeling and physiological deterioration after MI (29); however, no prominent changes in macrophages were found in our current study. One possible explanation is that the types of immune cells were simply the expression patterns inferred from genes.

Metabolic characterization of the myocardium suggests that cardiometabolic disturbances underlie most cardiovascular diseases. Untargeted mass spectrometry-based analysis found that changes in sphingomyelin metabolism were associated with cardiovascular diseases (30), suggesting that both immune and metabolic disorders are involved in the occurrence and development of MI. The link between metabolism and immune responses is not limited to MI but also has potential roles in other diseases. Sphingolipid signaling is involved in regulating the functions of immune cells including neutrophils, macrophages, NK cells, CD8^{+}

T cells, and CD4^{+} T cells. Recent evidence suggests that activation of the S1P pathway inhibits neutrophil apoptosis in acute lung injury (31). In contrast, neutrophil elastase has also been reported to increase neutrophil counts and airway ceramide levels in lung disease (32). One of the main metabolic pathways in MI is SM. A previous study has proposed that S1P-mediated signaling changes in the heart after MI have the *in vitro* potential to enhance cardiomyocyte survival and provide cardioprotection. Furthermore, SMs released by myocardial tissue during ischemic stress or inflammation may become therapeutic targets for cardiovascular diseases (33). It has been found that SM can be altered after MI by hydrolyzing ceramides in the heart, thereby supporting cardiac function by limiting neutrophil infiltration and altering the immune response (16).

In the identification of human DEGs, we found from

2994

Wang et al. Sphingolipid metabolism in immune cells

CIBERSORT and ClueGO that immune genes were significantly enriched in biological processes such as neutrophil migration and T cell activation/differentiation. Literature review and analyses of single-cell sequencing datasets further showed a correlation between neutrophils and SM. Therefore, in our current study, we explored the relationship between neutrophils and SM in MI. Six DEGs were found to be highly correlated with SM. Among them, *Asah1*, *Degs1*, and *Sptlc2* were significantly differentially expressed in neutrophils. Some enzymes are the products of these DEGs and can functionally achieve precise regulation of SMs and neutrophils.

Acid ceramidase (*Asah1*) is a key mature heterodimeric enzyme that regulates intracellular ceramide metabolism by catalyzing the hydrolysis of ceramides to sphingosine and fatty acids (34). Ceramides and sphingosines are important interconvertible SM metabolites that control multiple signaling pathways related to different aspects of cell survival and aging (35). It has been shown that high-mobility group box-1 (HMGB1) may damage the vasculature system through inhibition of *Asah1* and subsequent accumulation of long-chain ceramides in coronary cardiomyocytes (36). Ceramides are a class of lipids thought to be toxic, and their pathway enzymes are upregulated in ischemic myocardium, which may be one of the sources of plasma ceramide during MI (37). Furthermore, S1P generated by *Asah1* phosphorylation has been shown to inhibit inflammatory neutrophil recruitment and cardiomyocyte apoptosis and may stimulate tissue regeneration and improve cardiac function by attracting hematopoietic stem cells to the infarct site (38). The release of TNF-a, IL-1b, and IL-6 was significantly reduced in Asah1-overexpressing OBA9 cells (39). These results were generally consistent with our findings. The expression of the *Asah1* gene is downregulated in neutrophils, and insufficient *Asah1* expression will lead to the accumulation of ceramides and the reduction of S1P, resulting in the deterioration and remodeling of the myocardium after MI.

In the final step of *de novo* SM synthesis, a key gene, *Degs1*, encodes a desaturase that catalyzes the conversion of dihydroceramide to ceramide by adding a 4,5-trans-double bond (40). The levels of individual dihydroceramide and ceramide species as well as the ratios between species are associated with cardiovascular and metabolic diseases. Elevated ceramide level has been repeatedly shown to be associated with cardiovascular diseases. Gene expression analysis of *Degs1*-silenced cells revealed dramatic changes in cellular functions, including cell replication, intercellular

adhesion, and autophagy (41). A previous study showed that the expression level of *Degs1* was significantly increased in granulocyte-monocyte progenitors (GMPs) after 6 h of cytokine stimulation. Furthermore, it has been shown that subsequent activation of *Degs1* due to a sudden increase in *de novo* ceramide production may contribute to reperfusion cardiac injury (42). SPT is considered to be a heterodimer composed of 2 subunits, namely *Sptlc1* and *Sptlc2*. It is the rate-limiting enzyme for sphingolipid biosynthesis. A previous study showed that inhibition of SPT reduced ventricular remodeling, fibrosis, and macrophage content after MI, and deletion of the *Sptlc2* gene protected cardiac function after MI. In addition, SPT can also be activated by inflammatory responses by upregulating the expression of *Sptlc2* (43). It has been found that *Sptlc2* mediates antigenic stimulation and inflammatory signaling, modulates the SM of T cells, maintains the metabolic adaptation of CD8+ T cells, and supports protective immunity (44). Furthermore, neutrophil elastase may increase airway ceramide levels by increasing *Sptlc2* protein levels in mouse lungs (32).

Therefore, the pathogenesis of MI involves immune-metabolic disorders. These mechanisms include excessive accumulation of toxic or bioactive lipids as well as disruption of specific key cellular and physiological processes. The SM-related genes *Asah1*, *Degs1*, and *Sptlc2* are associated with neutrophils and may be potential therapeutic targets for MI. However, these results were obtained from a database-based analysis, and further studies are needed to determine their therapeutic potential in MI. The specific mechanisms by which these genes affect the inflammatory response in MI remain to be further validated experimentally. Our findings may contribute to a deeper understanding of the roles of metabolic genes in the pathogenesis of MI. Reprogramming SM to affect immune cells may become a new modality for MI protective therapy.

In summary, the discovery that the SM genes *Asah1*, *Degs1*, and *Sptlc2* are highly correlated with immune cell metabolism may deepen our understanding of metabolic genes in the pathogenesis of MI. Reprogramming SM to modulate immune cells may provide a new mode of protective therapy for MI. However, our results were derived from gene expression profiles. Further research and corresponding experimental verification are needed to clarify the specific mechanisms.

Acknowledgments

Footnote

Reporting Checklist: The authors have completed the STREGA reporting checklist. Available at https://jtd.amegroups.com/article/view/10.21037/jtd-22-1041/rc

Conflicts of Interest: All authors have completed the ICMJE uniform disclosure form (available at https://jtd.amegroups.com/article/view/10.21037/jtd-22-1041/coif). WW is from Guangzhou Xidai Hemodialysis Center Co., Ltd. The other authors have no conflicts of interest to declare.

Ethical Statement: The authors are accountable for all aspects of the work in ensuring that questions related to the accuracy or integrity of any part of the work are appropriately investigated and resolved. The study was conducted in accordance with the Declaration of Helsinki (as revised in 2013).

References

1. Thygesen K, Alpert JS, White HD, et al. Universal definition of myocardial infarction. Circulation 2007;116:2634-53.
2. Anderson JL, Morrow DA. Acute Myocardial Infarction. N Engl J Med 2017;376:2053-64.
3. Virani SS, Alonso A, Benjamin EJ, et al. Heart Disease and Stroke Statistics-2020 Update: A Report From the American Heart Association. Circulation 2020;141:e139-596.
4. Heusch G, Libby P, Gersh B, et al. Cardiovascular remodelling in coronary artery disease and heart failure. Lancet 2014;383:1933-43.
5. Ong SB, Hernández-Reséndiz S, Crespo-Avilan GE, et al. Inflammation following acute myocardial infarction: Multiple players, dynamic roles, and novel therapeutic opportunities. Pharmacol Ther 2018;186:73-87.
6. Szummer K, Wallentin L, Lindhagen L, et al. Improved outcomes in patients with ST-elevation myocardial infarction during the last 20 years are related to implementation of evidence-based treatments: experiences from the SWEDEHEART registry 1995-2014. Eur Heart J 2017;38:3056-65.
7. Andreadou I, Cabrera-Fuentes HA, Devaux Y, et al. Immune cells as targets for cardioprotection: new players and novel therapeutic opportunities. Cardiovasc Res 2019;115:1117-30.
8. Veiga-Fernandes H, Freitas AA. The S(c)ensory Immune System Theory. Trends Immunol 2017;38:777-88.
9. Brodin P, Davis MM. Human immune system variation. Nat Rev Immunol 2017;17:21-9.
10. Abnave P, Ghigo E. Role of the immune system in regeneration and its dynamic interplay with adult stem cells. Semin Cell Dev Biol 2019;87:160-8.
11. Maceyka M, Spiegel S. Sphingolipid metabolites in inflammatory disease. Nature 2014;510:58-67.
12. Hannun YA, Obeid LM. Sphingolipids and their metabolism in physiology and disease. Nat Rev Mol Cell Biol 2018;19:175-91.
13. Laaksonen R, Ekroos K, Sysi-Aho M, et al. Plasma ceramides predict cardiovascular death in patients with stable coronary artery disease and acute coronary syndromes beyond LDL-cholesterol. Eur Heart J 2016;37:1967-76.
14. Knapp M, Zendzian-Piotrowska M, Kurek K, et al. Myocardial infarction changes sphingolipid metabolism in the uninfarcted ventricular wall of the rat. Lipids 2012;47:847-53.
15. Klyachkin YM, Nagareddy PR, Ye S, et al. Pharmacological Elevation of Circulating Bioactive Phosphosphingolipids Enhances Myocardial Recovery After Acute Infarction. Stem Cells Transl Med 2015;4:1333-43.
16. Hadas Y, Vincek AS, Youssef E, et al. Altering Sphingolipid Metabolism Attenuates Cell Death and Inflammatory Response After Myocardial Infarction. Circulation 2020;141:916-30.
17. Reforgiato MR, Milano G, Fabriàs G, et al. Inhibition of ceramide de novo synthesis as a postischemic strategy to reduce myocardial reperfusion injury. Basic Res Cardiol 2016;111:12.
18. Hua T, Bao Q, He X, et al. Lipidomics Revealed Alteration of Sphingolipid Metabolism During the Reparative Phase After Myocardial Infarction Injury. Front Physiol 2021;12:663480.
19. Wixon J, Kell D. The Kyoto encyclopedia of genes and

genomes--KEGG. Yeast 2000;17:48-55.

20. Dennis G Jr, Sherman BT, Hosack DA, et al. DAVID: Database for Annotation, Visualization, and Integrated Discovery. Genome Biol 2003;4:P3.

21. Chen B, Khodadoust MS, Liu CL, et al. Profiling Tumor Infiltrating Immune Cells with CIBERSORT. Methods Mol Biol 2018;1711:243-59.

22. Amulic B, Cazalet C, Hayes GL, et al. Neutrophil function: from mechanisms to disease. Annu Rev Immunol 2012;30:459-89.

23. Liew PX, Kubes P. The Neutrophil's Role During Health and Disease. Physiol Rev 2019;99:1223-48.

24. Soehnlein O, Steffens S, Hidalgo A, et al. Neutrophils as protagonists and targets in chronic inflammation. Nat Rev Immunol 2017;17:248-61.

25. Espaillat MP, Snider AJ, Qiu Z, et al. Loss of acid ceramidase in myeloid cells suppresses intestinal neutrophil recruitment. FASEB J 2018;32:2339-53.

26. Seumois G, Fillet M, Gillet L, et al. De novo C16- and C24-ceramide generation contributes to spontaneous neutrophil apoptosis. J Leukoc Biol 2007;81:1477-86.

27. Kumar BV, Connors TJ, Farber DL. Human T Cell Development, Localization, and Function throughout Life. Immunity 2018;48:202-13.

28. Bai A, Guo Y. Acid sphingomyelinase mediates human CD4+ T-cell signaling: potential roles in T-cell responses and diseases. Cell Death Dis 2017;8:e2963.

29. Haider N, Boscá L, Zandbergen HR, et al. Transition of Macrophages to Fibroblast-Like Cells in Healing Myocardial Infarction. J Am Coll Cardiol 2019;74:3124-35.

30. Ganna A, Salihovic S, Sundström J, et al. Large-scale metabolomic profiling identifies novel biomarkers for incident coronary heart disease. PLoS Genet 2014;10:e1004801.

31. Lin WC, Lin CF, Chen CL, et al. Inhibition of neutrophil apoptosis via sphingolipid signaling in acute lung injury. J Pharmacol Exp Ther 2011;339:45-53.

32. Karandashova S, Kummarapurugu AB, Zheng S, et al. Neutrophil elastase increases airway ceramide levels via upregulation of serine palmitoyltransferase. Am J Physiol Lung Cell Mol Physiol 2018;314:L206-14.

33. Egom EE, Mamas MA, Clark AL. The potential role of sphingolipid-mediated cell signaling in the interaction between hyperglycemia, acute myocardial infarction and heart failure. Expert Opin Ther Targets 2012;16:791-800.

34. Lucki NC, Bandyopadhyay S, Wang E, et al. Acid ceramidase (ASAH1) is a global regulator of steroidogenic capacity and adrenocortical gene expression. Mol Endocrinol 2012;26:228-43.

35. Duarte C, Akkaoui J, Yamada C, et al. Elusive Roles of the Different Ceramidases in Human Health, Pathophysiology, and Tissue Regeneration. Cells 2020;9:1379.

36. Yuan X, Bhat OM, Lohner H, et al. Downregulation of Lysosomal Acid Ceramidase Mediates HMGB1-Induced Migration and Proliferation of Mouse Coronary Arterial Myocytes. Front Cell Dev Biol 2020;8:111.

37. de Carvalho LP, Tan SH, Ow GS, et al. Plasma Ceramides as Prognostic Biomarkers and Their Arterial and Myocardial Tissue Correlates in Acute Myocardial Infarction. JACC Basic Transl Sci 2018;3:163-75.

38. Ouyang J, Shu Z, Chen S, et al. The role of sphingosine 1-phosphate and its receptors in cardiovascular diseases. J Cell Mol Med 2020;24:10290-301.

39. Azuma MM, Balani P, Boisvert H, et al. Endogenous acid ceramidase protects epithelial cells from Porphyromonas gingivalis-induced inflammation in vitro. Biochem Biophys Res Commun 2018;495:2383-9.

40. Xie SZ, Garcia-Prat L, Voisin V, et al. Sphingolipid Modulation Activates Proteostasis Programs to Govern Human Hematopoietic Stem Cell Self-Renewal. Cell Stem Cell 2019;25:639-653.e7.

41. Blackburn NB, Michael LF, Meikle PJ, et al. Rare DEGS1 variant significantly alters de novo ceramide synthesis pathway. J Lipid Res 2019;60:1630-9.

42. Siddique MM, Li Y, Chaurasia B, et al. Dihydroceramides: From Bit Players to Lead Actors. J Biol Chem 2015;290:15371-9.

43. Ji R, Akashi H, Drosatos K, et al. Increased de novo ceramide synthesis and accumulation in failing myocardium. JCI Insight 2017;2:e82922.

44. Wu J, Ma S, Sandhoff R, et al. Loss of Neurological Disease HSAN-I-Associated Gene SPTLC2 Impairs CD8+ T Cell Responses to Infection by Inhibiting T Cell Metabolic Fitness. Immunity 2019;50:1218-1231.e5.

Table S1 Human differentially expressed genes

Serial Number	Gene symbol	logFC	AveExpr	t	P value	adj.P.Val	B
1	MMP9	2.33855	11.39744	3.592684	0.001447	0.114746	−0.99687
2	ORM1	2.050829	9.612759	3.123483	0.004583	0.141748	−1.99794
3	MCEMP1	1.843211	11.20557	3.45113	0.002057	0.120544	−1.30314
4	ARG1	1.784609	8.083946	3.848874	0.00076	0.101436	−0.43591
5	IL18R1	1.546932	8.643282	3.894366	0.000678	0.101436	−0.3356
6	PGLYRP1	1.517608	10.43151	3.255345	0.003328	0.132604	−1.72101
7	CAMP	1.496792	10.90982	3.698059	0.001111	0.111207	−0.76705
8	CA4	1.471609	10.05532	3.371215	0.002505	0.126349	−1.47458
9	S100A12	1.447968	10.74816	3.517834	0.001743	0.119091	−1.1592
10	FCGR3B	1.414302	10.88318	3.345398	0.00267	0.127775	−1.52972
11	ECHDC3	1.32054	8.421084	3.239501	0.003459	0.132997	−1.75449
12	IRAK3	1.317233	9.16895	4.264529	0.000265	0.089633	0.485366
13	FOLR3	1.304274	10.79752	2.285455	0.031317	0.276952	−3.63265
14	LOC642103	1.303792	8.672873	3.866846	0.000727	0.101436	−0.3963
15	ACSL1	1.292266	10.08229	4.218997	0.000297	0.090968	0.384079
16	DYSF	1.264499	11.86615	3.354106	0.002613	0.127223	−1.51113
17	PADI4	1.223377	12.28883	3.400366	0.002332	0.125287	−1.41218
18	HP	1.215895	7.322892	2.555381	0.017289	0.220023	−3.13463
19	IL18RAP	1.187086	11.17354	2.89503	0.007902	0.170773	−2.46727
20	PROK2	1.174429	12.98078	3.379069	0.002457	0.125916	−1.45778
21	PYGL	1.167348	10.19208	4.208486	0.000305	0.09124	0.360704
22	SIPA1L2	1.166231	8.489526	3.372887	0.002495	0.126349	−1.47101
23	CLEC4D	1.156188	7.405215	3.400546	0.002331	0.125287	−1.41179
24	ALPL	1.150232	13.00948	3.102799	0.004817	0.146188	−2.04101
25	ROPN1L	1.144992	9.448411	2.775595	0.010448	0.185178	−2.7065
26	LOC653117	1.139672	7.976339	3.381343	0.002444	0.125865	−1.45292
27	MANSC1	1.1275	8.222488	3.925216	0.000627	0.101436	−0.26748
28	ORF1-FL49	1.124751	10.18106	2.527126	0.018421	0.224676	−3.18823
29	GPR97	1.092025	8.383472	3.70988	0.001079	0.110079	−0.74118
30	MOSC1	1.089598	9.938144	2.587743	0.016072	0.213737	−3.07286
31	IRS2	1.083028	8.900794	3.284835	0.003097	0.130499	−1.65855
32	LMNB1	1.081206	8.473903	3.051433	0.005449	0.151332	−2.14749
33	CRISPLD2	1.080124	10.80395	3.099087	0.00486	0.146704	−2.04872
34	TGM3	1.073379	7.900303	3.012086	0.005987	0.154027	−2.22858
35	LOC349114	1.070626	10.82487	3.885659	0.000693	0.101436	−0.35481
36	LOC642342	1.067055	7.918864	2.690664	0.012712	0.197474	−2.87372

Table S1 (*continued*)

Table S1 (*continued*)

Serial Number	Gene symbol	logFC	AveExpr	t	P value	adj.P.Val	B
37	*LY96*	1.066468	10.98948	2.540627	0.017872	0.223087	–3.16266
38	*SLPI*	1.061257	9.046528	2.347527	0.027385	0.260869	–3.52101
39	*PFKFB3*	1.060199	9.432671	3.590107	0.001456	0.114746	–1.00248
40	*FLJ22662*	1.044749	12.46665	4.814163	6.49E–05	0.072264	1.707448
41	*GCA*	1.043038	12.59706	3.840441	0.000777	0.101436	–0.45448
42	*RGS2*	1.034452	13.15926	4.774309	7.19E–05	0.072264	1.619115
43	*FKBP5*	1.03339	10.41034	2.99846	0.006185	0.155473	–2.25657
44	*LOC399744*	1.027444	9.873342	3.205542	0.003757	0.135874	–1.82607
45	*CD55*	1.020389	9.603337	3.512764	0.001765	0.119091	–1.17017
46	*CHST13*	1.0201	9.805034	3.859619	0.00074	0.101436	–0.41223
47	*LTB4R*	1.017101	8.427242	3.84109	0.000775	0.101436	–0.45305
48	*CLEC4E*	1.015684	7.826687	3.224836	0.003585	0.134343	–1.78544
49	*ANXA3*	1.012378	7.051623	3.492685	0.001856	0.119091	–1.21355
50	*CKAP4*	1.003048	11.09385	3.659829	0.001223	0.11284	–0.85059
51	*FBXL13*	1.001643	7.691442	3.049857	0.00547	0.151332	–2.15074
52	*LILRA5*	0.993919	11.25931	2.982081	0.006431	0.156937	–2.29014
53	*B4GALT5*	0.985579	10.77976	3.920045	0.000635	0.101436	–0.2789
54	*F5*	0.985088	8.506003	3.077533	0.005119	0.14834	–2.09347
55	*CECR6*	0.983334	8.508134	3.040875	0.005589	0.152571	–2.16929
56	*HECW2*	0.974347	7.287907	3.734033	0.001015	0.110079	–0.68828
57	*FOS*	0.972587	9.229026	3.160815	0.004188	0.139303	–1.91995
58	*ANPEP*	0.968834	10.76946	3.968088	0.000562	0.101436	–0.17269
59	*Rgr*	0.968752	10.38948	2.849467	0.008795	0.17471	–2.55907
60	*DUSP1*	0.964046	12.76663	3.267508	0.003231	0.132009	–1.69527
61	*TGFA*	0.962063	7.720036	3.895929	0.000675	0.101436	–0.33215
62	*HIST2H2BE*	0.96044	9.031172	3.149621	0.004303	0.140679	–1.94337
63	*SLC22A15*	0.958536	8.101279	4.140758	0.000363	0.094589	0.21017
64	*HIST2H2AA3*	0.958347	11.41927	2.526451	0.018449	0.224676	–3.1895
65	*TLR4*	0.958101	9.18805	3.497562	0.001833	0.119091	–1.20302
66	*AQP9*	0.957989	13.50962	3.712842	0.001071	0.110079	–0.7347
67	*HIP1*	0.953096	8.115247	3.471373	0.001956	0.119761	–1.25953
68	*LOC653371*	0.951121	8.661355	3.065774	0.005265	0.149166	–2.11783
69	*LOC441268*	0.947782	9.152189	2.677494	0.013101	0.199505	–2.89942
70	*CPD*	0.944102	9.406912	3.686689	0.001144	0.111784	–0.79192
71	*CEACAM4*	0.943713	8.086616	3.108249	0.004754	0.145229	–2.02967

Table S1 (*continued*)

Table S1 (*continued*)

Serial Number	Gene symbol	logFC	AveExpr	t	P value	adj.P.Val	B
72	*TCN1*	0.942214	8.782168	2.662482	0.013559	0.202119	−2.92864
73	*OSM*	0.940691	7.529336	3.310247	0.00291	0.13001	−1.60458
74	*TLR5*	0.9373	9.745737	2.224044	0.035706	0.290852	−3.74129
75	*CYP1B1*	0.928915	8.373661	2.7382	0.011394	0.190756	−2.78044
76	*NFIL3*	0.91496	8.251641	3.790872	0.00088	0.105508	−0.56354
77	*SLC22A4*	0.913925	9.018558	2.858914	0.008602	0.173889	−2.54009
78	*CEBPD*	0.913613	12.84609	4.185639	0.000323	0.094254	0.309906
79	*SLC2A3*	0.911516	12.96729	4.23495	0.000285	0.090936	0.419561
80	*STX3A*	0.910053	10.36261	3.500865	0.001818	0.119091	−1.19589
81	*VNN3*	0.904921	8.367341	2.903752	0.007741	0.16946	−2.44962
82	*HMFN0839*	0.904171	9.416283	3.731334	0.001022	0.110079	−0.6942
83	*NCF4*	0.902133	10.30241	3.242633	0.003433	0.132997	−1.74788
84	*ADM*	0.901671	11.53919	2.720281	0.011875	0.192873	−2.8157
85	*USP10*	0.897881	9.908695	3.070616	0.005205	0.148634	−2.1078
86	*SRPK1*	0.89357	9.879312	3.21476	0.003674	0.134737	−1.80667
87	*UTS2*	0.89268	7.466917	2.293205	0.030799	0.275231	−3.61881
88	*HIST1H4H*	0.890945	8.298639	2.247953	0.033934	0.284635	−3.69922
89	*PANX2*	0.889438	9.056248	2.738672	0.011381	0.190756	−2.77951
90	*DIRC2*	0.888298	9.092107	4.495556	0.000147	0.073882	0.999631
91	*CDA*	0.883487	10.95916	2.366729	0.026264	0.255022	−3.48611
92	*GNG10*	0.882075	9.877978	2.135861	0.042985	0.314615	−3.89399
93	*HIST2H2AC*	0.880485	10.70033	2.116317	0.044768	0.320232	−3.92729
94	*MEGF9*	0.870553	7.462872	3.647392	0.001262	0.114131	−0.87773
95	*NALP12*	0.870473	9.429302	3.294857	0.003022	0.13001	−1.63728
96	*ANKRD22*	0.866808	7.806823	2.091595	0.047119	0.325772	−3.96912
97	*BASP1*	0.866505	13.59508	3.210976	0.003708	0.135202	−1.81464
98	*LRG1*	0.865795	10.32178	2.230758	0.0352	0.289141	−3.72951
99	*HDAC4*	0.864611	7.852802	5.971405	3.50E−06	0.02969	4.214237
100	*LCN2*	0.858625	9.709791	2.186425	0.038662	0.300859	−3.80692
101	*HK3*	0.858413	10.87087	3.339833	0.002706	0.127775	−1.54159
102	*C20orf3*	0.85739	9.96218	3.855664	0.000747	0.101436	−0.42095
103	*HMGB2*	0.85678	8.647755	3.526271	0.001707	0.119091	−1.14095
104	*SLC11A1*	0.856464	9.66204	4.154234	0.00035	0.094589	0.240109
105	*CACNA1E*	0.854318	7.068674	2.796587	0.009951	0.183124	−2.66479
106	*FLJ10357*	0.850417	8.179703	2.517423	0.018826	0.226444	−3.20656
107	*RGS18*	0.849717	10.83583	2.528825	0.018351	0.224447	−3.18501

Table S1 (*continued*)

Table S1 (*continued*)

Serial Number	Gene symbol	logFC	AveExpr	t	P value	adj.P.Val	B
108	*PGS1*	0.843711	10.6579	3.190727	0.003895	0.13781	−1.85722
109	*RNF149*	0.839186	10.8767	4.102777	0.000399	0.094872	0.125826
110	*TLR2*	0.834368	7.769845	3.133922	0.004469	0.140679	−1.97617
111	*BCL3*	0.830419	9.508695	3.516308	0.00175	0.119091	−1.1625
112	*LOC651738*	0.829173	8.173647	3.380254	0.00245	0.125865	−1.45525
113	*C5AR1*	0.829085	11.39232	3.519138	0.001738	0.119091	−1.15638
114	*NQO2*	0.827101	8.705838	2.393281	0.024783	0.247391	−3.43757
115	*LOC648984*	0.825385	8.314506	2.456283	0.021571	0.237028	−3.32116
116	*BST1*	0.824826	8.677447	3.54254	0.001639	0.119011	−1.10571
117	*CARD12*	0.822336	8.238939	2.88128	0.008162	0.172597	−2.49504
118	*CD58*	0.820587	9.266517	3.209518	0.003721	0.135487	−1.81771
119	*SCAP2*	0.819857	10.25521	3.675176	0.001177	0.11284	−0.81708
120	*EDG4*	0.818534	10.21035	3.725269	0.001038	0.110079	−0.70749
121	*ST3GAL4*	0.81817	7.943227	2.811939	0.009601	0.180616	−2.63419
122	*RP2*	0.817528	8.197989	3.165505	0.00414	0.138695	−1.91013
123	*KIAA0963*	0.817423	8.600882	4.303627	0.000239	0.086915	0.572373
124	*ATP6V0B*	0.816517	10.80856	4.647073	9.95E−05	0.072264	1.336648
125	*IL8RA*	0.815445	10.92273	2.205822	0.037111	0.296365	−3.77317
126	*VMD2*	0.814589	9.436611	3.188833	0.003913	0.13781	−1.86119
127	*GYG1*	0.814114	10.64613	2.786892	0.010178	0.18372	−2.68407
128	*LILRA2*	0.813957	10.97871	3.413718	0.002256	0.124185	−1.38354
129	*HSDL2*	0.813921	8.427604	4.422547	0.000177	0.077928	0.837108
130	*FRAT1*	0.812065	9.123137	3.467144	0.001977	0.119799	−1.26865
131	*LENG4*	0.811355	11.25982	2.875466	0.008274	0.172831	−2.50677
132	*FPRL1*	0.809264	10.06055	2.135609	0.043007	0.314615	−3.89442
133	*LOC653610*	0.808777	7.849722	2.674543	0.01319	0.200124	−2.90517
134	*SLC26A8*	0.808734	7.209328	3.754901	0.000964	0.109803	−0.64252
135	*SIGLEC5*	0.807663	9.032474	2.259584	0.033102	0.282028	−3.67865
136	*PELI1*	0.805934	10.1023	2.630817	0.014575	0.206774	−2.99
137	*FLJ20273*	0.804335	7.948573	3.34768	0.002655	0.127775	−1.52485
138	*ITGAM*	0.804079	10.26273	4.274804	0.000258	0.089633	0.50823
139	*MCTP2*	0.803754	8.006926	2.475112	0.020688	0.233066	−3.28603
140	*RNF24*	0.802888	11.40401	2.430368	0.022843	0.241087	−3.36925
141	*C19orf35*	0.802216	7.512469	3.198327	0.003824	0.136676	−1.84125
142	*TMCO3*	0.799679	8.596421	3.235518	0.003493	0.133108	−1.7629
143	*ABHD5*	0.798541	8.840811	2.884112	0.008108	0.172444	−2.48933

Table S1 (*continued*)

Table S1 (*continued*)

Serial Number	Gene symbol	logFC	AveExpr	t	P value	adj.P.Val	B
144	LOC283547	0.796563	6.979395	3.085916	0.005017	0.148163	−2.07608
145	PGD	0.796243	12.43107	3.02764	0.005769	0.152905	−2.19657
146	GALNAC4S-6ST	0.794714	12.07299	4.086112	0.000417	0.097888	0.088838
147	HAL	0.791353	7.854326	3.588907	0.00146	0.114746	−1.00509
148	CEACAM8	0.790408	7.227308	2.160284	0.040845	0.307581	−3.8521
149	TRIB1	0.790401	10.38493	3.331937	0.002759	0.128564	−1.55842
150	FPR1	0.789551	14.02212	3.022161	0.005845	0.153245	−2.20786
151	ALOX5AP	0.788982	14.17016	3.04984	0.00547	0.151332	−2.15078
152	FLJ25084	0.787961	8.288837	2.615201	0.015102	0.208688	−3.02012
153	PLSCR1	0.786905	7.58977	2.431621	0.022779	0.24098	−3.36693
154	JUNB	0.786169	9.570536	3.808319	0.000842	0.103855	−0.52518
155	ST6GALNAC2	0.784136	7.339946	3.219228	0.003634	0.134343	−1.79726
156	SLA	0.780878	9.781019	4.020426	0.000492	0.100639	−0.05682
157	UBTD1	0.780731	8.694828	3.17565	0.00404	0.138527	−1.88886
158	TMEM71	0.77993	11.81099	3.131734	0.004493	0.140679	−1.98073
159	FAM101B	0.777627	9.381775	2.135291	0.043036	0.314615	−3.89497
160	SERPINB1	0.777571	11.38287	3.553948	0.001593	0.118763	−1.08098
161	EGFL5	0.777044	8.019667	2.700761	0.01242	0.19555	−2.85397
162	CBS	0.777002	7.359541	2.913399	0.007567	0.168443	−2.43008
163	CD14	0.775077	13.21877	3.144077	0.004361	0.140679	−1.95496
164	GK	0.774984	9.489446	2.529121	0.018339	0.224447	−3.18445
165	MAN2A2	0.774488	8.667437	3.946366	0.000594	0.101436	−0.22073
166	FLJ14166	0.774291	7.939962	2.680868	0.013001	0.198921	−2.89284
167	PLXDC2	0.771475	8.572042	3.922366	0.000631	0.101436	−0.27377
168	BPI	0.771469	7.534782	2.540305	0.017885	0.223087	−3.16327
169	CSTA	0.76932	8.007036	3.308855	0.00292	0.13001	−1.60754
170	SLC16A3	0.767409	11.81859	3.695624	0.001118	0.111228	−0.77238
171	GALNT4	0.76721	8.397417	3.56302	0.001558	0.118188	−1.0613
172	CXCL16	0.765991	10.76887	2.838703	0.009019	0.176046	−2.58066
173	LOC441124	0.763976	9.846763	2.587283	0.016088	0.213737	−3.07374
174	LOC654053	0.763413	7.554788	3.011772	0.005991	0.154027	−2.22923
175	LOC642788	0.762867	8.126854	2.460962	0.021348	0.236628	−3.31244
176	C13orf18	0.760816	8.824058	3.131949	0.00449	0.140679	−1.98028
177	GPR84	0.754246	7.04973	2.093948	0.046891	0.325595	−3.96515
178	IFNGR1	0.753636	11.93233	3.498854	0.001827	0.119091	−1.20023
179	HIATL1	0.752146	9.014104	2.713344	0.012066	0.193839	−2.82931

Table S1 (*continued*)

Table S1 (*continued*)

Serial Number	Gene symbol	logFC	AveExpr	t	P value	adj.P.Val	B
180	STX11	0.750366	11.07139	3.418071	0.002232	0.123858	−1.3742
181	TM6SF1	0.750293	9.074907	3.285801	0.003089	0.130499	−1.6565
182	ZNF337	−0.75001	8.944149	−3.89277	0.00068	0.101436	−0.33911
183	HLA-DOA	−0.75121	8.854112	−2.7093	0.012179	0.194513	−2.83725
184	CRIP2	−0.75402	7.938499	−2.80485	0.009761	0.182009	−2.64833
185	DHRS3	−0.76111	7.560627	−4.57363	0.00012	0.07266	1.173348
186	DDX24	−0.76164	9.5677	−3.45037	0.002061	0.120544	−1.30478
187	LOC644191	−0.76648	11.60427	−2.1134	0.04504	0.321093	−3.93225
188	ITM2C	−0.76671	8.808128	−3.21965	0.003631	0.134343	−1.79637
189	GPR18	−0.76798	8.580795	−3.29302	0.003035	0.13001	−1.64118
190	LOC649821	−0.76866	12.18526	−4.34341	0.000216	0.085544	0.660921
191	LOC648622	−0.76885	12.38212	−2.42633	0.023047	0.241494	−3.37671
192	C12orf57	−0.76978	10.85188	−2.45594	0.021587	0.237028	−3.32179
193	CD8A	−0.77619	9.906367	−2.14767	0.041938	0.31125	−3.87378
194	RPS4X	−0.77764	12.59376	−4.58514	0.000117	0.072273	1.198957
195	LDHB	−0.7803	9.831459	−3.3253	0.002805	0.128834	−1.57255
196	LOC653328	−0.78121	11.54146	−2.58571	0.016146	0.213737	−3.07675
197	MAL	−0.78541	10.23088	−3.25921	0.003297	0.132604	−1.71283
198	NCR3	−0.78655	8.6003	−4.07074	0.000433	0.098004	0.054725
199	IL32	−0.7885	9.697537	−3.29887	0.002992	0.13001	−1.62876
200	TRIB2	−0.79006	8.616554	−3.27235	0.003193	0.131465	−1.68502
201	RPS26L	−0.80172	9.984061	−2.16061	0.040818	0.307581	−3.85155
202	RARRES3	−0.80229	12.14882	−3.91124	0.000649	0.101436	−0.29835
203	CD247	−0.80416	12.53859	−2.61872	0.014982	0.208558	−3.01334
204	CD160	−0.80476	7.630201	−2.8499	0.008786	0.17471	−2.5582
205	DENND2D	−0.80589	10.49128	−4.06855	0.000436	0.098004	0.049877
206	MCOLN2	−0.8083	8.435576	−3.05842	0.005359	0.150297	−2.13304
207	HLA-DOB	−0.81102	9.184469	−3.02014	0.005873	0.153245	−2.21201
208	LOC652694	−0.81194	8.906794	−3.4075	0.002291	0.12472	−1.39688
209	FAIM3	−0.81297	11.41093	−2.53416	0.018133	0.224029	−3.17492
210	MGC3020	−0.81448	8.61429	−3.33919	0.002711	0.127775	−1.54296
211	LOC387841	−0.81572	10.90099	−3.41888	0.002228	0.123858	−1.37247
212	SPOCK2	−0.81583	11.48066	−2.43969	0.022377	0.239905	−3.35199
213	FLT3LG	−0.81864	8.565727	−3.96973	0.00056	0.101436	−0.16906
214	LEF1	−0.82094	9.720332	−2.4076	0.024016	0.244978	−3.41127
215	SCAP1	−0.82256	9.78988	−3.30548	0.002944	0.13001	−1.61472

Table S1 (*continued*)

Table S1 (*continued*)

Serial Number	Gene symbol	logFC	AveExpr	t	P value	adj.P.Val	B
216	LOC127295	−0.8237	11.05735	−3.01575	0.005935	0.154027	−2.22104
217	PYHIN1	−0.82801	8.57903	−3.67382	0.001181	0.11284	−0.82003
218	HLA-DRB4	−0.83001	9.804237	−2.08442	0.047822	0.327511	−3.9812
219	GPR114	−0.83279	8.701368	−3.51195	0.001769	0.119091	−1.17192
220	OLIG2	−0.83652	7.032241	−2.86931	0.008395	0.173523	−2.51918
221	ITGB7	−0.84304	10.60249	−2.72643	0.011707	0.192328	−2.80361
222	LOC644928	−0.84845	12.01624	−2.11775	0.044635	0.320067	−3.92485
223	BIN1	−0.84878	10.46447	−2.65717	0.013725	0.202912	−2.93897
224	LOC643516	−0.85382	10.55106	−2.11633	0.044767	0.320232	−3.92727
225	CD52	−0.86105	13.39095	−2.83007	0.009203	0.177193	−2.59795
226	LIME1	−0.86457	11.40487	−3.04563	0.005526	0.151332	−2.15947
227	STAT4	−0.86504	10.11262	−2.86657	0.008449	0.173523	−2.52469
228	RPS28	−0.86668	11.05779	−3.57501	0.001512	0.116446	−1.03527
229	FAM113B	−0.86692	10.50775	−3.37445	0.002485	0.126349	−1.46766
230	CD6	−0.86788	10.77341	−2.51923	0.01875	0.226163	−3.20314
231	LOC643284	−0.87404	12.79172	−2.88229	0.008142	0.172594	−2.49299
232	GNLY	−0.87674	10.39489	−2.98901	0.006325	0.15623	−2.27595
233	LOC642113	−0.88218	11.39643	−2.58006	0.016353	0.214761	−3.08757
234	IL2RB	−0.88978	10.01101	−2.6445	0.014128	0.205409	−2.96353
235	CD3E	−0.89182	9.240109	−3.40738	0.002292	0.12472	−1.39714
236	LOC642989	−0.89314	8.880034	−2.61208	0.015209	0.209055	−3.02612
237	NKG7	−0.89625	13.57092	−3.2727	0.00319	0.131465	−1.68428
238	EVL	−0.90372	11.21729	−3.08501	0.005028	0.148163	−2.07797
239	GIMAP5	−0.91102	11.0163	−3.42257	0.002207	0.123604	−1.36453
240	ADA	−0.91273	9.50594	−4.79111	6.89E−05	0.072264	1.656368
241	IL7R	−0.92035	11.78686	−2.43755	0.022483	0.240018	−3.35595
242	PTPRCAP	−0.92261	10.19472	−3.47458	0.001941	0.119761	−1.25261
243	CD2	−0.93005	11.42993	−2.88619	0.008068	0.172444	−2.48513
244	CD3G	−0.93782	8.864575	−3.4053	0.002304	0.125093	−1.4016
245	LOC647450	−0.95568	10.74394	−2.66039	0.013624	0.202613	−2.93271
246	GZMA	−0.97496	11.37146	−2.78657	0.010185	0.18372	−2.68472
247	MGC2463	−0.97563	9.552363	−3.6642	0.00121	0.11284	−0.84105
248	PLEKHF1	−0.97819	9.699774	−3.97975	0.000546	0.101436	−0.1469
249	GZMM	−0.98612	9.379308	−3.19303	0.003873	0.13781	−1.85238
250	LOC652493	−0.98652	11.02899	−2.9173	0.007498	0.168225	−2.42216
251	KSP37	−1.01331	11.36509	−2.76829	0.010627	0.186609	−2.72099

Table S1 (*continued*)

Table S1 (*continued*)

Serial Number	Gene symbol	logFC	AveExpr	t	P value	adj.P.Val	B
252	*LOC648470*	−1.03568	7.946623	−3.21255	0.003694	0.135095	−1.81133
253	*PRSS33*	−1.05323	7.198497	−3.21936	0.003633	0.134343	−1.79698
254	*HLA-DQB1*	−1.06138	8.66443	−2.68635	0.012838	0.198399	−2.88214
255	*GZMH*	−1.07345	11.7948	−2.85642	0.008653	0.174282	−2.54511
256	*EDG8*	−1.10221	9.526576	−3.71701	0.00106	0.110079	−0.72558
257	*EOMES*	−1.15728	9.752873	−3.82151	0.000815	0.103009	−0.49615
258	*KLRB1*	−1.23806	11.15357	−3.67055	0.001191	0.11284	−0.82717
259	*HLA-DQA1*	−1.2628	11.61509	−3.74374	0.000991	0.109803	−0.66701
260	*CLC*	−1.30502	12.16514	−2.9172	0.007499	0.168225	−2.42237
261	*GZMK*	−1.52524	10.44113	−4.25723	0.000269	0.090115	0.469134

Table S2 Mouse differentially expressed genes

Serial Number	Genes	logFC	AveExpr	t	P value	adj.P.Val	B
1	Crct1	2.863021	4.541184	9.395201	8.28E-11	5.19E-08	14.67284
2	Spp1	2.730707	7.270417	6.485436	2.43E-07	1.23E-05	6.916784
3	Arg1	2.710166	4.543406	7.775877	6.25E-09	8.16E-07	10.48345
4	Timp1	2.640296	8.895089	9.662649	4.19E-11	3.89E-08	15.3298
5	Hmox1	2.224186	6.971768	9.441278	7.36E-11	5.19E-08	14.78675
6	Sprr1a	2.156611	5.695751	9.880761	2.42E-11	3.37E-08	15.85803
7	Lox	2.127652	7.464368	8.578265	7.04E-10	1.99E-07	12.60373
8	Plac8	2.054676	6.841903	7.879555	4.69E-09	7.69E-07	10.76207
9	Clec4d	1.920933	6.825022	7.73988	6.90E-09	8.77E-07	10.38641
10	S100a8	1.900213	8.304187	8.388319	1.17E-09	2.83E-07	12.10945
11	Ch25h	1.887793	7.219974	8.174944	2.09E-09	4.07E-07	11.54845
12	Adamts4	1.886303	5.629356	11.85892	2.21E-13	4.91E-10	20.34267
13	Ctgf	1.79361	11.16576	12.49802	5.37E-14	2.23E-10	21.67741
14	Lgals3	1.762002	8.590551	7.074251	4.48E-08	3.59E-06	8.564998
15	Tyms-ps	1.72692	4.174637	5.254638	8.94E-06	0.000204	3.409753
16	Gdf15	1.703975	6.146522	8.645897	5.88E-10	1.82E-07	12.77855
17	S100a9	1.603418	7.673497	7.333169	2.15E-08	2.05E-06	9.279339
18	Birc5	1.582838	5.535746	5.082996	1.48E-05	0.000297	2.920381
19	Ccnb1	1.574293	4.074561	7.328454	2.18E-08	2.06E-06	9.266394
20	Tubb6	1.565439	8.80278	15.62173	1.01E-16	1.13E-12	27.48084
21	Ms4a6d	1.550032	7.544527	7.165099	3.46E-08	3.03E-06	8.81644
22	Rcan1	1.547355	8.331236	9.568952	5.32E-11	4.55E-08	15.1008
23	Col8a1	1.532879	7.558911	6.879442	7.82E-08	5.21E-06	8.02308
24	Pbk	1.51785	5.784307	7.049321	4.81E-08	3.77E-06	8.495855
25	Socs3	1.507867	7.916062	5.41593	5.56E-06	0.00014	3.87049
26	Gadd45g	1.497063	8.399149	9.376997	8.68E-11	5.19E-08	14.62776
27	Ptx3	1.443862	6.518	3.304621	0.002314	0.014713	−1.91934
28	Crlf1	1.443747	4.898414	4.755652	3.86E-05	0.00061	1.991904
29	Nppb	1.425335	12.05621	4.858024	2.86E-05	0.000483	2.281397
30	Ccl2	1.413387	6.707517	8.147412	2.25E-09	4.32E-07	11.47563
31	Hbegf	1.409587	8.120138	7.066631	4.58E-08	3.64E-06	8.543872
32	Ccl7	1.39941	7.613086	6.921326	6.94E-08	4.81E-06	8.139896
33	Tnc	1.382189	5.410614	8.257777	1.67E-09	3.54E-07	11.76695
34	Uck2	1.375348	8.150792	12.36756	7.13E-14	2.23E-10	21.40931
35	2810417H13Rik	1.375077	5.335933	7.012427	5.35E-08	4.05E-06	8.393413
36	Egr2	1.327421	5.814	4.472583	8.79E-05	0.001154	1.197143
37	Actn1	1.311669	8.556536	9.7018	3.80E-11	3.84E-08	15.42512

Table S2 (*continued*)

Table S2 (*continued*)

Serial Number	Genes	logFC	AveExpr	t	P value	adj.P.Val	B
38	*Ccl4*	1.309986	5.788751	7.279936	2.50E-08	2.30E-06	9.13305
39	*Fos*	1.282655	7.729037	2.706016	0.010735	0.050444	–3.34175
40	*Slc15a3*	1.262459	6.203595	8.895063	3.04E-10	1.22E-07	13.41716
41	*Ccl3*	1.262315	4.877557	5.115091	1.35E-05	0.000277	3.011789
42	*Il1r2*	1.233537	5.456273	4.735057	4.10E-05	0.00064	1.933782
43	*Saa3*	1.232552	6.851739	3.072109	0.004263	0.024169	–2.49045
44	*Hspa1b*	1.231091	6.203991	2.859575	0.007333	0.037279	–2.99241
45	*Enpp1*	1.22163	6.21141	7.426072	1.66E-08	1.66E-06	9.533894
46	*Fcgr4*	1.215886	6.535248	4.726474	4.20E-05	0.00065	1.909574
47	*Ppbp*	1.197468	6.543436	5.045916	1.65E-05	0.00032	2.814844
48	*Kif23*	1.191204	5.569109	6.397251	3.14E-07	1.49E-05	6.667542
49	*Lpxn*	1.189445	6.220901	7.778038	6.21E-09	8.16E-07	10.48928
50	*Cytip*	1.171651	6.183458	6.723399	1.22E-07	7.56E-06	7.586475
51	*Mcm5*	1.166037	6.179141	6.385352	3.25E-07	1.52E-05	6.63387
52	*Col5a1*	1.142503	8.798087	6.236744	5.01E-07	2.05E-05	6.212607
53	*Cdca7*	1.140553	5.773233	5.542628	3.83E-06	0.000103	4.232693
54	*Tnfrsf12a*	1.133759	9.13381	6.249417	4.83E-07	2.00E-05	6.248583
55	*Fpr2*	1.132524	5.605523	5.537601	3.89E-06	0.000104	4.218321
56	*Ckap2*	1.118768	4.401823	3.901159	0.00045	0.004125	–0.36928
57	*Hspa1a*	1.117219	6.138667	2.901123	0.006604	0.034358	–2.8959
58	*Emp1*	1.111437	10.54126	12.31397	8.02E-14	2.23E-10	21.29853
59	*Fkbp11*	1.110746	6.31651	7.839829	5.23E-09	7.92E-07	10.65547
60	*Kif22*	1.105788	5.864035	6.603314	1.73E-07	9.62E-06	7.249075
61	*Cd68*	1.104017	7.343844	6.454261	2.66E-07	1.31E-05	6.828733
62	*Cyr61*	1.096554	7.173034	3.734036	0.000718	0.005927	–0.81409
63	*Fcer1g*	1.094929	9.316485	6.900649	7.36E-08	4.99E-06	8.082247
64	*Cdca3*	1.084787	4.952785	7.168243	3.43E-08	3.03E-06	8.825128
65	*Car13*	1.079713	4.531785	3.920346	0.000427	0.00395	–0.31776
66	*Serpinb1a*	1.073001	5.752773	4.923687	2.36E-05	0.000418	2.467541
67	*Serpina3n*	1.070749	9.336211	3.911884	0.000437	0.004026	-0.34049
68	*Col3a1*	1.068191	8.229082	4.59133	6.23E-05	0.000878	1.529396
69	*Atf3*	1.064302	7.041239	2.732205	0.010066	0.04769	–3.28301
70	*Lcn2*	1.063186	9.543997	3.134905	0.003621	0.021219	–2.33835
71	*Kif2c*	1.055171	4.982798	6.631339	1.60E-07	9.26E-06	7.327921
72	*Fstl1*	1.052578	9.50243	6.021627	9.39E-07	3.46E-05	5.600697
73	*Cd52*	1.051972	7.382433	6.301166	4.15E-07	1.84E-05	6.395391

Table S2 (*continued*)

Table S2 (*continued*)

Serial Number	Genes	logFC	AveExpr	*t*	P value	adj.P.Val	B
74	Anxa2	1.049522	10.46118	9.755248	3.32E-11	3.76E-08	15.55489
75	Trem2	1.049392	5.07342	3.443959	0.001591	0.011056	−1.56732
76	Serpina3g	1.048026	6.035373	4.667295	5.00E-05	0.000738	1.742848
77	Mfap5	1.039535	8.793577	6.105384	7.35E-07	2.87E-05	5.839208
78	Il1b	1.01851	5.927251	5.989383	1.03E-06	3.70E-05	5.508797
79	Tgfbi	1.016335	8.172203	7.946361	3.90E-09	7.00E-07	10.94089
80	Cd276	1.015765	5.686277	5.353892	6.67E-06	0.000163	3.693207
81	Psat1	1.015662	6.058616	7.801128	5.83E-09	8.10E-07	10.55144
82	Cxcl1	1.013593	7.589755	2.750973	0.009611	0.046039	−3.2407
83	Fignl1	1.008587	4.605079	4.573049	6.57E-05	0.000916	1.478129
84	Mmp12	1.003598	4.301818	4.166051	0.000212	0.002317	0.349193
85	Cd72	1.001706	5.562123	3.363725	0.001975	0.012993	−1.77086
86	Slpi	1.001176	5.384753	5.256997	8.87E-06	0.000204	3.416488
87	Hp	0.99122	5.808328	5.379427	6.19E-06	0.000152	3.766171
88	Kdelr3	0.987952	6.985439	5.412844	5.61E-06	0.000141	3.861671
89	Plk1	0.985449	5.340773	4.613853	5.84E-05	0.000832	1.592614
90	Cotl1	0.984346	7.513187	6.544911	2.05E-07	1.10E-05	7.08457
91	D17H6S56E-5	0.981083	5.858928	8.300349	1.49E-09	3.35E-07	11.87889
92	Bub1b	0.978041	4.694523	3.051754	0.004494	0.025206	−2.53939
93	Tpm4	0.961758	9.591386	9.747577	3.38E-11	3.76E-08	15.53629
94	Prc1	0.960467	5.43594	5.631822	2.95E-06	8.47E-05	4.487705
95	Selp	0.951039	5.54268	3.382415	0.001879	0.012573	−1.72365
96	Coro1a	0.948905	6.729098	8.891098	3.07E-10	1.22E-07	13.40706
97	Rgs16	0.945256	5.012616	5.617627	3.07E-06	8.76E-05	4.447122
98	Sphk1	0.944083	6.014605	3.233231	0.002796	0.017175	−2.09696
99	Ncaph	0.941184	5.830927	6.72512	1.22E-07	7.56E-06	7.591302
100	Meox1	0.937791	7.608033	5.446527	5.08E-06	0.00013	3.957948
101	Angptl4	0.937013	6.737262	8.737916	4.60E-10	1.55E-07	13.01539
102	Gsg2	0.931685	3.576241	2.714874	0.010504	0.049507	−3.32192
103	Fgl2	0.928781	7.668162	4.191688	0.000197	0.002184	0.419494
104	Csrp2	0.928252	8.973758	5.589632	3.34E-06	9.30E-05	4.367083
105	Clec4n	0.927169	6.323797	5.424501	5.42E-06	0.000137	3.894987
106	Col1a2	0.925749	8.300465	4.259092	0.000163	0.00188	0.604904
107	Plek	0.92041	6.014536	6.641966	1.55E-07	9.11E-06	7.357801
108	Itga5	0.919707	6.211585	8.562035	7.35E-10	1.99E-07	12.56169
109	Mns1	0.91524	4.458898	3.723093	0.00074	0.006046	−0.84295

Table S2 (*continued*)

Serial Number	Genes	logFC	AveExpr	t	P value	adj.P.Val	B
110	*Sparc*	0.914699	10.45404	6.949625	6.40E-08	4.53E-06	8.218732
111	*Ankrd1*	0.912801	12.17731	6.295966	4.22E-07	1.85E-05	6.380646
112	*E2f1*	0.910321	4.956115	5.027207	1.74E-05	0.000334	2.761621
113	*Ctss*	0.907766	7.521755	6.122708	6.99E-07	2.74E-05	5.888502
114	*Plaur*	0.906797	6.032381	6.085602	7.79E-07	2.96E-05	5.782905
115	*Col4a1*	0.902328	11.16531	11.01655	1.54E-12	2.85E-09	18.49962
116	*Mest*	0.901592	5.694265	6.519793	2.20E-07	1.15E-05	7.013741
117	*Uhrf1*	0.888688	5.020161	5.944071	1.18E-06	4.18E-05	5.379588
118	*Glipr1*	0.887341	6.288346	7.451994	1.54E-08	1.59E-06	9.604748
119	*Slc11a1*	0.886028	6.618615	8.487166	8.98E-10	2.32E-07	12.36728
120	*Sh3bgrl3*	0.884478	9.223618	6.287021	4.33E-07	1.87E-05	6.35528
121	*Arc*	0.882257	4.909133	2.384307	0.023076	0.091101	−4.0329
122	*Ltb4r1*	0.875155	4.723035	3.259514	0.002608	0.016226	−2.0318
123	*Slfn1*	0.8739	4.653378	3.592665	0.001061	0.007997	−1.18439
124	*Il33*	0.873818	7.125471	4.988583	1.95E-05	0.000362	2.651816
125	*Fxyd5*	0.872004	8.285237	8.314804	1.43E-09	3.31E-07	11.91685
126	*Cxcl10*	0.865217	4.875396	4.50498	8.01E-05	0.001073	1.287607
127	*Eif1a*	0.862412	7.748776	8.314656	1.43E-09	3.31E-07	11.91646
128	*Rab15*	0.862088	5.823859	4.238725	0.000173	0.001978	0.548795
129	*Fn1*	0.861186	6.416267	6.623088	1.63E-07	9.42E-06	7.304714
130	*Ncf4*	0.859503	6.0911	6.367419	3.43E-07	1.57E-05	6.583108
131	*Nfkbiz*	0.858683	6.939325	5.096461	1.42E-05	0.000288	2.958725
132	*Aldh1a2*	0.851614	6.075972	7.055121	4.73E-08	3.73E-06	8.511946
133	*Dbf4*	0.849003	5.215327	7.620181	9.63E-09	1.13E-06	10.06259
134	*Wisp2*	0.845709	6.695483	3.921968	0.000425	0.003942	−0.3134
135	*Ccl9*	0.84432	9.325856	5.826243	1.67E-06	5.42E-05	5.043288
136	*Phlda1*	0.840003	9.197087	4.665161	5.03E-05	0.00074	1.736844
137	*Dpysl3*	0.83587	7.71842	6.987461	5.74E-08	4.29E-06	8.324017
138	*Rab32*	0.835324	6.250527	3.807114	0.000586	0.005029	−0.62047
139	*Cstb*	0.83415	10.15037	6.608722	1.70E-07	9.62E-06	7.264295
140	*Cdc20*	0.833531	5.685693	6.037888	8.96E-07	3.31E-05	5.647025
141	*Fscn1*	0.832561	7.563563	5.651716	2.78E-06	8.14E-05	4.544578
142	*Laptm5*	0.831623	9.280225	6.376185	3.34E-07	1.54E-05	6.607925
143	*Slc2a1*	0.82368	8.470273	6.366232	3.44E-07	1.57E-05	6.579748
144	*Fstl3*	0.822875	5.630903	10.66545	3.54E-12	5.62E-09	17.70248
145	*Tubb2b*	0.822845	5.781533	7.680615	8.14E-09	9.84E-07	10.2263

Table S2 (*continued*)

Table S2 (*continued*)

Serial Number	Genes	logFC	AveExpr	t	P value	adj.P.Val	B
146	Ier3	0.819429	9.767533	6.449043	2.70E-07	1.32E-05	6.813988
147	Akr1b8	0.81518	6.810862	6.556248	1.98E-07	1.08E-05	7.116524
148	Cdt1	0.814889	5.506507	6.96822	6.07E-08	4.36E-06	8.270493
149	Kif4	0.812222	3.943529	3.581565	0.001094	0.00815	−1.21322
150	Tagln2	0.810407	9.55806	6.543613	2.06E-07	1.10E-05	7.08091
151	Fen1	0.802585	6.899571	4.282024	0.000152	0.001788	0.668167
152	Cd14	0.800306	7.658858	6.330888	3.81E-07	1.72E-05	6.479639
153	Sdc4	0.797291	7.685882	5.888392	1.39E-06	4.71E-05	5.220724
154	Slc39a6	0.796369	6.819033	8.971364	2.49E-10	1.15E-07	13.611
155	Cdkn1a	0.792997	8.469194	3.706966	0.000774	0.006268	−0.88544
156	Pdlim7	0.78905	8.12009	6.453479	2.67E-07	1.31E-05	6.826525
157	Ankrd2	0.788656	4.850389	2.982194	0.005374	0.02911	−2.70529
158	Thbs1	0.787275	5.504342	3.01841	0.004897	0.027045	−2.61918
159	Col16a1	0.786462	7.322472	5.831355	1.64E-06	5.37E-05	5.057887
160	Aurkb	0.784888	4.505715	4.323567	0.000135	0.001623	0.783001
161	B4galnt1	0.78401	4.367177	5.220906	9.87E-06	0.00022	3.313487
162	Mcam	0.783949	7.122872	8.29564	1.50E-09	3.35E-07	11.86652
163	Tmsb10	0.781764	8.559025	5.744621	2.12E-06	6.54E-05	4.81012
164	Mcm6	0.780565	6.337901	7.882973	4.65E-09	7.69E-07	10.77123
165	Gbx2	0.778426	4.251346	3.475001	0.001463	0.010305	−1.48797
166	Cttnbp2nl	0.778221	6.455769	6.968021	6.07E-08	4.36E-06	8.269939
167	Adora2b	0.777036	5.488061	6.485153	2.44E-07	1.23E-05	6.915983
168	Nme1	0.776988	9.688281	7.476426	1.44E-08	1.54E-06	9.671459
169	Cxcl2	0.776887	5.121122	2.354913	0.024687	0.09588	−4.09307
170	Rasl11b	0.775792	9.511824	5.223056	9.80E-06	0.00022	3.319622
171	Rhoc	0.775536	7.919184	8.913847	2.89E-10	1.22E-07	13.46495
172	Ifi30	0.773195	6.916198	5.387724	6.04E-06	0.000149	3.789878
173	Mfap4	0.772569	6.195811	2.169485	0.03742	0.131593	−4.46024
174	Endod1	0.77169	6.03429	5.376094	6.25E-06	0.000153	3.756645
175	Cdr2	0.768676	7.488368	9.398751	8.21E-11	5.19E-08	14.68163
176	1810055G02Rik	0.768092	7.502752	8.747639	4.48E-10	1.55E-07	13.04035
177	Alox5ap	0.762873	8.750718	5.575924	3.47E-06	9.59E-05	4.32789
178	Skap2	0.761715	7.87022	7.495652	1.36E-08	1.47E-06	9.723909
179	Top2a	0.760622	4.777575	6.487356	2.42E-07	1.23E-05	6.922205
180	Fcrls	0.759945	7.790314	4.001511	0.000339	0.003312	−0.09889
181	Fcgr1	0.758774	5.662569	4.685251	4.74E-05	0.000712	1.793397

Table S2 (*continued*)

Table S2 (*continued*)

Serial Number	Genes	logFC	AveExpr	t	P value	adj.P.Val	B
182	*Sh3bp2*	0.7582	6.12335	6.139284	6.66E-07	2.63E-05	5.935655
183	*Adam8*	0.756025	5.166035	5.040421	1.68E-05	0.000323	2.799211
184	*Tyrobp*	0.752886	7.768627	4.798126	3.41E-05	0.000548	2.111902
185	*Vav1*	0.752155	5.342631	3.695439	0.000799	0.006415	−0.91576
186	*Adipoq*	−0.7534	4.771748	−2.62145	0.013186	0.059187	−3.52897
187	*Cdkn1c*	−0.79062	8.094014	−6.09002	7.69E-07	2.95E-05	5.795474
188	*Ift81*	−0.79523	9.236377	−6.26005	4.68E-07	1.96E-05	6.278759
189	*G0s2*	−0.80085	8.667639	−5.90565	1.32E-06	4.49E-05	5.269987
190	*Tcf15*	−0.85034	7.409164	−9.37001	8.84E-11	5.19E-08	14.61044
191	*Hmgcs2*	−0.91996	6.42425	−6.24632	4.87E-07	2.00E-05	6.239801
192	*Cfd*	−1.07267	6.57724	−2.60548	0.013703	0.061065	−3.56391
193	*Ano10*	−1.30361	8.872708	−8.6946	5.16E-10	1.65E-07	12.90405
194	*Inmt*	−1.38816	7.497009	−6.85599	8.36E-08	5.50E-06	7.957602